Study of imaging Photoplethysmogram (iPPG) for non-contact Pulse Rate Measurement

A DISSERTATION

SUBMITTED IN PARTIAL FULFILLMENT OF THE REQUIREMENTS
FOR THE AWARD OF THE DEGREE
OF

MASTER OF TECHNOLOGY
IN
SIGNAL PROCESSING AND DIGITAL DESIGN

Submitted by:

SHIVANGI NANGIA
2K20/SPD/12

Under the supervision of

PROF. AJAI KUMAR GAUTAM

Assistant Professor

DEPARTMENT OF ELECTRONICS AND COMMUNICATION ENGINEERING
DELHI TECHNOLOGICAL UNIVERSITY
(Formerly Delhi College of Engineering)
Bawana Road, Delhi-110042

MAY, 2022

DEPARTMENT OF ELECTRONICS AND COMMUNICATION ENGINEERING
DELHI TECHNOLOGICAL UNIVERSITY
(Formerly Delhi College of Engineering)
Bawana Road, Delhi-110042

CANDIDATE'S DECLARATION

I, **SHIVANGI NANGIA**, an MTech (Signal Processing and Digital Design) student, hereby declare that the project Dissertation titled "**Study of imaging Photoplethysmogram (iPPG) for non-contact Pulse Rate Measurement**," which I submitted to the Department of Electronics and Communication Engineering, Delhi Technological University, Delhi in partial fulfillment of the criteria for the granting of a Master of Technology degree, is original and not duplicated from any source. A degree, diploma, associateship, or fellowship has not previously been awarded based on this work's merits.

Place: Delhi   **SHIVANGI NANGIA**
Date: May 20, 2022

DEPARTMENT OF ELECTRONICS AND COMMUNICATION ENGINEERING

DELHI TECHNOLOGICAL UNIVERSITY
(Formerly Delhi College of Engineering)
Bawana Road, Delhi-110042

<u>CERTIFICATE</u>

This Project Dissertation, titled "**Study of Imaging Photoplethysmogram (iPPG) for Non-Contact Pulse Rate Measurement**," submitted by **SHIVANGI NANGIA**, **2K20/SPD/12** of the Electronics and Communication Department, Delhi Technological University, Delhi, is a record of the project work done by students under my supervision. To the best of my knowledge, this work has never been submitted for consideration for a degree or diploma at either this university or the other.

Place: Delhi

PROF. AJAI KUMAR GAUTAM

Date: May 20, 2022

SUPERVISOR

<u>ABSTRACT</u>

In this thesis, I have studied about non-contact detection of pulse rate, pertaining to the recent covid times. Heart rate is a reliable measure of an individual's current physiological state, which includes studies of cognitive and emotional state, as well as routine health exams, for human beings. Heart rate can be estimated non-invasively via pulse rate, which is connected with changes in the optical characteristics of the skin tissue (imaging Photoplethysmogram, iPPG). However, there is no well-established approach for measuring pulse rates in awake and behaving animals that is easy and non-invasive. On a public dataset, this study aims to provide an algorithmic framework for comparing techniques of pulse rate estimate utilizing imaging photoplethysmography (iPPG). In this article, we outline the key processes in the calculation of pulse rate from facial video and discuss the methodologies used at each stage.

An analysis of signal processing algorithms for heart rate estimation, important parameters, and a comparison to industry standards are all included in the study. Using a simple, low-cost, multi-purpose screening method like this one allows us to gain relevant information about heart rate. As a result, heart rate monitoring can be used for mass screening in a cost-effective and offer significant benefits, making this technology attractive.

ACKNOWLEDGEMENT

A successful project can never be prepared by the efforts of the person to whom the project is assigned, but it also requires the aid and guardianship of individuals who helped in completion of the project.

I would want to thank all those persons who have assisted me in my research and encouraged me during my studies.

I owe a debt of appreciation to my Research Supervisor, Prof. Ajai Kumar Gautam, for his encouragement, support, patience, and advice. Furthermore, I would also want to thank Prof. Rajiv Kapoor, who provided me the right to utilize the essential equipment and the appropriate format to complete the dissertation.

I give my sincerest appreciation to my family - my mother and father who have always stood by me and supported me through my profession, and have pushed me through against impossible circumstances at times. No words can adequately explain how grateful I am to them. The thesis would have been finished a month earlier if it weren't for my friends at Delhi Technological University.

SHIVANGI NANGIA

Table of Contents

List of Tables

List of Figures

List of Abbreviations

MMIR Multi-Modal Image Registration

MI Mutual Information

LC Left Canthi

RC Right Canthi

FH Fore Head

SD Standard Deviation

FPS Frames per Second

IPPG Image Photoplethysmography

CC Correlation Coefficient

SSD Sum of Squared Difference

PPG Photo Plethysmography

POS Plane Orthogonal to Skin

WHO Word Health Organization

ICA Independent Component Analysis

JADE Joint Approximation Diagonalization of Eigen matrices

Chapter 1: Introduction

1.1 Overview

As indicated by a gauge from World Health Organization (WHO), pandemic from infections like Ebola, H5N1 bird flu could kill up to 100 million individuals [2]. Moderating danger of such irresistible pandemics might be conceivable through mass fever separating public places, for example, air terminals, clinics and boundary crossing focuses [7, 12]. Fever is one of the normal symptomatic manifestations, which can be utilized to contain the scourge through seclusion of patients and clinical consideration. If there should arise an occurrence of irresistible sicknesses episode, a fast and proficient screening process is expected to recognize contaminated patients. Early manifestations of diseases can be recognized through irregularities in internal heat level and pulse. Customary techniques for estimating such human essential signs are intrusive, tedious and work escalated [34,44]. To empower mass screening, we want gadgets/strategies that are harmless, practical, simple to introduce and have the option to recognize patients with fever [29]. A few investigations [18] show that IRTGs empower a reasonable and harmless mass screening approach through recognition of raised temperatures. IRTGs have been utilized effectively as a device for mass fever screening of SARS 2003 flare-up [29,30]. Research in this space is essential as plagues like Ebola, bird influenza, zika are relied upon to hit 20 to 30 % of total populace. Global Organization for Standardization (ISO) meeting in 2005 at IEC-DIN Germany, examined Standard Technical Reference [29, 40] to empower acknowledgment of infrared imaging in clinical applications.

This thesis tries to throw light on late procedures of IPPG which research utilization of practical techniques for pulse checking utilizing recorded video of the subject. This empowers contact free estimation of human imperative signs a good way off from the subject, which is exceptionally engaging for mass fever screening application. These detached imaging techniques empower long haul checking of fundamental signs with next to no burden to the patients.

Studies incorporate foundation data about signal handling calculations for assessing pulse, pertinent boundaries and correlation with standard procedures. Such minimal expense, multi-reason answers for speedy screening of subjects give us reasonable and valuable data about internal heat level and pulse.

Irregularities in internal heat level and pulse are obvious signs of disease. These estimations can be utilized for screening such tainted subjects. These new turns of events in research show promising outcomes that empower us to utilize customer grade gadgets as practical symptomatic apparatuses for assessment of internal heat level or heart beat rate through thermograms and recorded recordings individually.

1.2 Contributions of Thesis

This proposition investigates various techniques for enrollment of apparent and IR face pictures to empower temperature estimation utilizing inward canthi. Particularly for a human face, which is non-unbending, relative models are restricted in exactness for enlistment. We carry out a free structure deformity (FFD)- based enrollment strategy to further develop the enlistment exactness after relative change. The improvement in enrollment precision utilizing relative and deformable changes is analyzed. We likewise assess the plausibility of enlistment based programmed temperature estimation as an option in contrast to manual estimation. A total execution for enrollment of apparent and IR pictures through relative and deformable changes in MATLAB (The MathWorks. Inc.) is given.

Also, the review researches the utilization of minimal expense (portable camera/Digital Camera) video recording gear in surrounding light for non-contact pulse assessment. The recorded video utilizing RGB shading space with webcam/versatile camera shows pulse throbs in green channel which shows most noteworthy retention. Changes in surrounding light and programmed splendor change in such video recording gadgets have huge in effect on the underlining PPG signal. The review depends on manual division to investigate various ROIs for pulse assessment. Bland Altman and connection analysis are also used to assess the presentation's quality, as are standard deviation and root mean square blunder (RMSE). The proposal also focuses on a variety of boundaries, such as the ROI area, the range examination window size, and the casing rate. This empowers us to diagram the necessities and their effect on pulse assessment utilizing IPPG.

1.3   Outline of Thesis

The heart rate is a good predictor of an individual's current anatomic condition, with purposes ranging from experimental examinations of cognitive and emotional state to thorough health exams. Non-contact assessment of pulse rate is possible in humans due to changes in the ocular residences in skin tissue, where cardiac cycles are supplied. Despite this, there is no easy and non-invasive alternative to heart rate monitoring in the huge human population. The primary goal of this is to provide an algorithmic framework for integrating several ways of heart rate monitoring utilizing (iPPG) imaging photoplethysmography, and to investigate the overall representation of various current tactics on an openly available dataset. The thesis is coordinated as follows. Chapter 2 gives foundation data on picture photoplethysmography (IPPG). Chapter 3 portrays the exploratory arrangement, input recordings, outline of IPPG calculation and results for pulse assessment. Chapter 4 gives ends drawn from test results.

Chapter 2: Theory

2.1 Image Photoplethysmography (IPPG)

Plethysmography steams from Greek work plethysmos meaning varieties in size attributable to blood flow. Customary plethysmography measures pulsativity in tissue volume and blood abundance straightforwardly through strain check. Electrocardiograms are now the gold standard for estimating heart rate (ECG). It requires the patient to wear adhesive gel patches or chest lashes, which may cause skin irritation or pain. The monetarily accessible heartbeat oximetry, which are by and large joined to fingers or ear projections are badly arranged for subjects and can cause torment over long term. Accessibility of a remote and non-contact based observing or evaluating frameworks for cardiovascular movement is a fascinating possibility for essential medical services and observation. Pavlidis et. al. [17] exhibited a methodology for estimating of physiological boundaries through face and warm recordings.
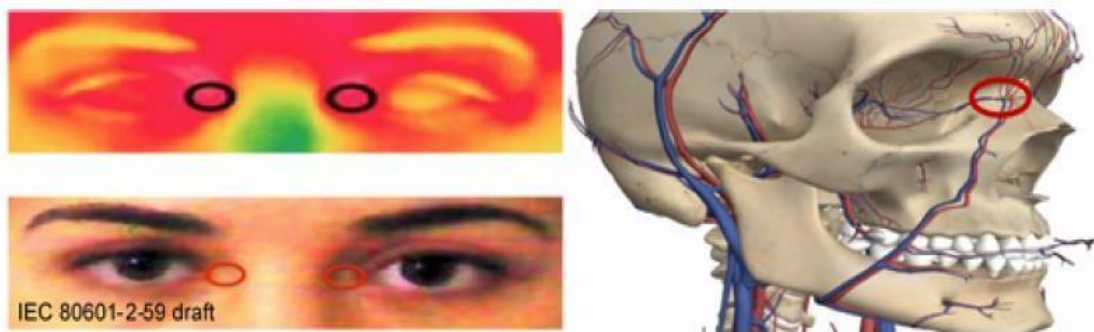

Figure 2.1: Canthi regions for screening (IEC 80601-2-59:2008) [1]

Figure 2.2: The canthi regions (a: IR image; b: white-light image) [9]

Photograph Plethysmography (PPG) is a minimal expense and harmless method for detecting cardiovascular heartbeat by estimating the variety in communicated or mirrored light through tissues [38]. Such strategies may not give the subtleties of

cardiovascular electrical conduction as in ECG; however, they give helpful data on heart beat rate by getting brief term recordings in an unhindered and agreeable way.

Regularly, traditional PPG has a committed light source, which can be comprehensively classified into two sorts: PPGs in both transmission and reflection modes are available. Using an LED light source and a photodetector on either side, transmission mode PPG calculates how light is repelled and retained through tissues. Reflectance mode PPG has the LED and photodetector on similar side and studies how much light reflected from a tissue surface.

The fundamental PPG signal in such plethysmographs is a complicated capacity of physiological boundaries, estimation philosophy and actual properties of sensor. Non-contact picture PPG (IPPG), is a kind of reflectance mode PPG which utilizes video accounts with encompassing light sources.

It is a functioning field of exploration, offering bits of knowledge into execution of painless human imperative sign observing [42]. The essential guideline of IPPG depends on association of encompassing light with natural tissues. Like customary PPG signals, it is a mind-boggling capacity of physiological boundaries, securing framework and the properties of light dissipating.

The light collaborations with organic tissues bring about force adjustment in the recorded video which is coordinated with heart beat. There are numerous characteristic parts that impact this vacillation in powers like blood volume, vein divider development and the direction of the red platelets. One of the primary donors of such varieties is blood stream and volumetric change in vein because of development of circulatory system.

The assimilation range inside shading range for frequency length of 450-700 nm for (1) oxyhaemoglobin (HbO2) and (2) deoxygenated haemoglobin (Hb) as displayed in Fig. 2.5. The green light shows top ingestion and red shows the most minimal assimilation, which is approved in view of perceptions from exploratory outcomes. Such painless assessments of cardiovascular movement are valuable in reconnaissance to assessed irregularities in heart beat rate.
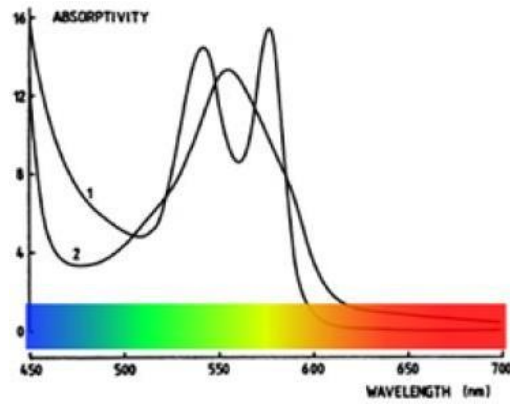
Figure 2.3: Absorption spectrum of Haemoglobin within 450 nm to 700 nm
wavelength range [49]

Chapter 3: Imaging Photoplethysmography (IPPG)

3.1 Overview

Non-contact IPPG has made headway over the most recent couple of years towards checking fundamental signs through shopper grade video recording. This addresses a huge headway in clinical strategies for observing imperative signs. Conventional techniques incorporate contact-based strategies forestalling long haul patient checking. Non-contact IPPG is broadly explored because of its plausibility and minimal expense applications. The earliest examination on IPPG was accounted for in 2005, which talks about extraction of PPG signal from subject's wrist [47]. These were the first tests towards getting PPG signals from a camcorder. Comparable investigations were led with LED brightening and CMOS cameras coordinated at subjects' internal arm [15]. Later in 2008, a paper exhibited the extraction of PPG signals through video recording in encompassing light with business grade cameras utilizing quick Fourier change (FFT). This is utilized to extricate the pulse recurrence from blended recurrence content of video, giving extension to possible use in clinical setting [45]. Poh et al. [39] distributed papers that analysed utilizing a standard webcam incorporated into their PC, to separate PPG signal from subjects of various skin tones [39]. Many such investigations concentrated on assessment of PPG signal with advanced cameras, cell phones [42] and webcams [5].

This is a reasonable pattern in the expected application and numerous endeavours are being made to involve these techniques in clinical arrangement. Non-contact reflectance mode IPPG utilizes surrounding light and are showing promising bits of knowledge into eventual fate of non-contact fever screening and numerous different applications [45]. It gives harmless/distant estimation of heart beat, without the utilization of any cathodes. In non-contact PPG signal is separate from traditional purchaser grade video recording gear. The physiological boundaries, similar to heart and respiratory rates, can be extricated involving video recording gear to film the brilliance varieties in someone's skin. The basic rule for the noticed sign is a mind-boggling capacity of blood volume, volumetric change in veins and other physiological boundaries, which is a functioning area of exploration.

Notwithstanding, the brief span of video arrangement and direct model suspicion has displayed to give sensible outcomes [45] for pulse assessment. Thus, a presentation

assessment of attainability and exactness of these techniques across various boundaries is a fascinating review, which empowers wide scope of utilizations. This large number of techniques include video accounts for various subjects under surrounding light with a length of 30 seconds to few moments. In the event of IPPG accounts utilizing a RGB shading space, green channel shows clear pulse throbs where the assimilation is most elevated [49]. The normal of red, green and blue channels inside ROI across outlines gives a crude sign, which shows adjustment with pulse. The adjustment of mirrored surrounding light relies upon the colours in the skin, bone, and blood move through veins. An unmistakable pattern in the ingestion when blood volume changes in conduits and arterioles. This shows a PPG signal as AC signal regulated over a DC part. These reflection forces are exceptionally delicate movement relics and show helpless sign to-clamour proportion (SNR). Besides, unique picture handling calculations utilized in the video obtaining framework have significant impact on the exhibition of pulse assessment. This work studies the performs of IPPG for various edge rates and various ROI.

Pulse is a significant mark of psycho-enthusiastic state, practical status, and ailments overall. Customarily, pulse is likewise removed from (ECG) electrocardiogram else assessed by beat rate for example number of heartbeat signals sent from heart to fringe per second, as a rule exceptionally corresponded with pulse which can be registered from circuitous estimations, for example, Photoplethysmogram (PPG). Nonetheless, the two methods warrant contact sensors, as of which they could be disadvantageous, though non-contact pulse assessment is valuable, for instance, for recognizing driver sluggishness or unusual state.

In the event that pulse is of interest, however no other ECG boundaries, a minimal expense option in contrast to electrocardiogram is given by PPG i.e., Photoplethysmogram. Varieties of light mirrored via skin, is used in Photoplethysmogram which connect changes of blood bushel in the microvascular doss of skin tissue. Photoplethysmogram permits very precise assessment of heartbeat rate. For some, applications, beat rate is an adequate intermediary for pulse, the last option of which can be, stringently talking, just surveyed from direct cardiovascular estimations, like ECG. A contact sensor is needed in a customary PPG which encompasses light source in order to enlighten the skin as well as a photodetector to gauge revamps in mirrored light, which can be utilized for clinical reasons like beat oximeters. In assimilation to the traditional PPG, (iPPG) Imaging Photoplethysmogram

has been presumed as a non-contact and remote option for the people. (iPPG) Imaging Photoplethysmogram is gained utilizing a camcorder rather than a photodetector, under devoted or encompassing light. As of which the video is typically recorded via face locales or palms.

The imaging photoplethysmogram (iPPG) has been proposed as a non-contact method of assessing heart rate. IPPG follows the same pattern as contact PPG, however instead of using a simple camera locator to capture an image, a camcorder is used. Then, at that point, iPPG is registered from a succession of pictures, normally obtained from face or palm locales.
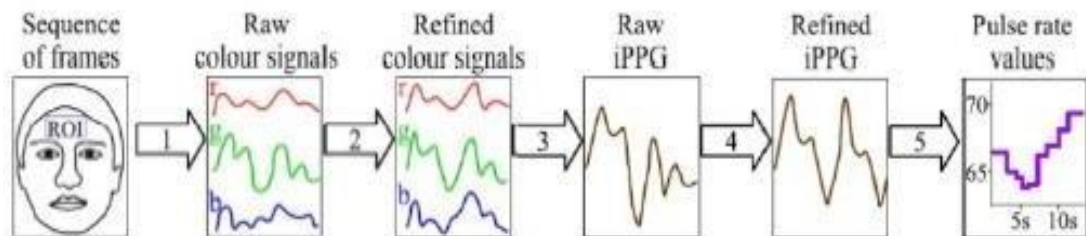
Figure 3.1: Pulse Rate Estimation using Facial Videos [15]

3.2 Methodology

3.2.1 Informational Collection Portrayal

The Dataset for Feeling Investigation utilizing EEG, Physiological and video signals contain physiological accounts and front facing face recordings of 25 human contributes viewing music recordings in 50 single minute preliminaries. The informational index for testing utilized was separated from the relative's accounts to different everyday circumstances and afterward the prepared code was physically tried on this dataset.

Recordings were gained under controlled light utilizing a One Or more Nord Portable Camera. After recording in MP4 format, the videos were transcoded to AVI format using the h264 codec to produce 50 FPS defused video. 720 x 586 was the target of the several recordings.

The sign was then registered at 512 Hz followed by down sampling to 256 Hz. After analysts determine each fragment using running mean over a 1-second window, we next sifted the data using the second request Butterworth channel, which we used in comparison to our preliminary choices of (PPG) Photoplethymogram segments to use.. Then, at that point, we processed reference beat rate esteems from PPG Photoplethysmogram, as reverse spans between diastolic minima were recognized consequently utilizing this technique.

Our investigation of heartbeat rate assessment comprised of ten exploratory meetings. We have attempted a few procurement boundaries to see whether they influence the iPPG quality, however didn't notice any significant distinction. When it comes to tactics and results, the RGB video has it all. A monochrome close infrared (NIR) video was also obtained as a control for the analysis of NIR and RGB video beat rate measurements. All movies were captured using ambient (non-dedicated) light. We utilized distinctive light conditions since setting a specific enlightenment is regularly unrealistic in ordinary circumstances, and we needed our video-based way to deal with have the option to adapt to this inconstancy. The table connected underneath clarifies the preparation informational index and contains a definite portrayal of the people present in the preparation recordings.

Sessions	Age, Full Years	Weight, Kg	Illumination	Luminance Cd/m^2
1,2	16	55.0	Fluorescent	87.5
3,4	8	35.5	Fluorescent + Daylight	12.6
5,6,9,10	11	45.0	Fluorescent + Daylight	12.9
7	12	50.5	Halogen + Daylight	4.0
8	10	42.0	Fluorescent + Daylight	12.7

Table 3.1: Detailed Information about Training Data Set [8]

3.2.2 Investigation

Facial recordings of people were handled to figure iPPG signals. The discrete Fourier transform of iPPG signal was taken into account for assessing beats from video PR of iPPG we figured via sliding covering windows in which every window beat rate is

assessed using the recurrence with most elevated plentifulness in the pulse transmission capacity, that is 80±100 beats per minute for people. A window of 1024 focuses was used in the DFT for all videos except video 2, which had a video outline rate of 1024 focuses. A larger window will result in a dismal transitory goal, while a more modest window will result in a more consistent rough goal. Using a heartbeat oximeter CAPNOX we obtained reference pulse rate values utilizing a test appended to the pointer of a human. This heartbeat oximeter doesn't give an information recording choice, yet it distinguishes heartbeats and presentations on the screen a worth of heartbeat rate registered as a converse of the normal between beat span in the course of the last 10 seconds. On the contrary the beat oximeter estimates beat rate within reach 20±240 beats per minute with an archived precision of ± 4 beats per minute. The beat oximeter screen was captured all the while with the individual's heart rate and facial video was separated and also disconnected from the video.

Frame Rate (fps)	Video Resolution (pixels)	Distance to human face (cm)	Session Duration (seconds)	Epoch Duration (seconds)
30	1920 x 1080	25	420	34.1
50	1920 x 1080	50	307	34.1
50	1280 x 1024	30	275	20.5
100	640 x 512	30	160	20.5
50	1280 x 1024	30	204	20.5
50	640 x 512	30	93	20.5
50	1280 x 1024	30	500	20.5
50	1280 x 1024	30	140	20.5

Table 3.2: Detailed Information of Data Set[10]

Method Choosing and Refining the area important to lessen spatially uncorrelated commotion and to upgrade the pulsatile signal, we arrived at the midpoint of upsides of shading channels over the return on initial capital investment. To choose pixels

containing most extreme measure of pulsatile data, we utilized the accompanying three-venture calculation:

1. A rectangular limit for the return for capital invested was chosen physically for the principal edge of the video. Since no noticeable movement was normal from a head-settled human, this limit continued as before for the entire video. It was found that the best iPPG extraction was for the nose and cheeks district 3 of the six heuristic regions that we tested.

2. Since hair, eyes, teeth, and so forth give no pulsatile data and weaken nature of the obtained iPPG, just skin pixels ought to comprise the return on initial capital investment. To recognize pixels comprising skin and no skin, casings were changed from the RGB to the HSV shading model as suggested. All pixels compassing likewise H, S or V were rejected, which were worth outside a predetermined reach. Via manual change supervised by visual control of the subsequent pixel region, three HSV ranges depicting human skin under various brightening conditions were chosen as shown in Table 3.1

3. Likewise, for each casing we avoided all exception pixels that contrasted altogether from different pixels in the return on initial capital investment. The point of this progression was to dispose of pixels undermined by antiquities. If the value of any shading channel ($ck^{i,j}$) would be less than the imbalance, we avoided the kth outline pixel (I, j).

$$M_k - 1.5\ \sigma_k < c_k^{i,j} < M_k + 1.5\ \sigma_k \qquad\qquad (3.1)$$

here σ_k and M_k are the standard deviation and mean of shading channel c stated for pixels of the kth outline; the coefficient 1.5 was chosen in light of the past work in this field.

3.2.3 Choosing Region of Interest

Shading powers $c_{i,j}$ (t) are arrived at the midpoint of over return on initial capital investment to process shading signals c0 (t) by (1). PPG-initiated variations of face tone have no effect on commotion or antiquities, hence the basis for selecting a region of interest is to select pixels with the most pulsatile data, which accumulates to reduce commotion while preserving the (iPPG) imaging. Photoplethysmogram signal. Region of interest comprises of the following steps: starting decision of facial area for

iPPG obtaining (return for capital invested decision) and barring insignificant pixels (return for money invested refinement).

3.2.3.1 Choice for Region of Interest

The most well-known methodology is to take a rectangular return on initial capital investment enveloping the entire face. Other famous districts are the entire face barring eye area and forehead. In DEAP dataset for certain members EEG covered the vast majority of the brow, which impeded utilizing the temple locale; accordingly, we thought about the entire face locale and the area of the face beneath the eyes. Following the two takes we recognized facial square shapes for all the particular edges by utilizing course classifier developed through the Viola-Jones calculation. We took the width of return on initial capital investment equivalent to 80 percentage of the assessed face width as suggested.

3.2.3.2 Refinement for Region of Interest

In any event, when area of liking is chosen appropriately, there will still be a few pixels which may not contain iPPG signal. Models incorporate pixels containing no skin (for example, hair, teeth etc), under or over lit regions and harmed pixels. To bar such pixels, area of interest refinement techniques is utilized, here we thought about two of them. To start with, pixels comprising no skin were disposed of. This was a fundamental piece of region of interest advancement for DEAP since in numerous recordings links hung before members' appearances, were viewed as containing no skin and disposed off (ranges were chosen exactly to give compelling skin determination to the whole dataset).

3.2.3.3 Pre-handling of shading signals

Upon this progression refined shading signals d (t) are processed from crude signs d0 (t) for u=1, K, T by smothering commotion and antiques. In order to protect applicable data, recurrence parts in human pulse transfer speed (50–250 beats per minute) was not required to be smothered. Following are the pre-handling sub-steps: detrending, band-pass and normal sifting. They are frequently utilized in blend, yet few of the sub-steps could be overlooked or processed at post-handling.

Detrending is significant because the pulsatile part of imaging Photoplethysmogram (iPPG) has significantly less abundancy compared to the gradually changing standard. A straightforward detrending technique comprises in mean-centring with scaling. Band-pass sifting smothers recurrence parts outside the pulse data transfer capacity. Here we utilized two generally utilized channels, either the 255th request limited motivation reaction (FIR) channel with straight stage planned utilizing the Hamming window or the fifth request Butterworth boundless drive reaction channel.

3.2.3.4 Post-handling of imaging Photoplethysmogram

Post-handling works on nature of imaging Photoplethysmogram (iPPG) signal. It becomes particularly vital when the clamour and antiquities are not eliminated in the pre-handling (Stage 2) or on the other hand in case iPPG was removed at Stage 3 in a non-straight manner. The post-handling sub-steps of band-pass, MA, and adaptive bandpass filtering are all discussed here. Band-pass and MA filtering described in the pre-handling substeps might also be used in post-handling, resulting in a variety of iPPG signals for all investigated extraction methods, except for straight G and GRD procedures. It is assumed that the frequency of recurrence components of the imaging Photoplethysmogram (iPPG) signal relating to the heart rate has a little stronger force; at that point, weaker parts compare to uproar and should be suppressed. We used a two-venture wavelet to separate the proposed. As a first step, we utilized iPPG's constant wavelet change to arrange wavelet coefficients, and then we measured the middle value of a 15-second transient running window by comparing it to the limit of squared wavelet coefficients. Then, at that point, we applied the standard Gaussian channel. The sifted signal was remade by playing out the opposite consistent wavelet change.

3.2.3.5 Assessment of Heartbeat rate

We consider here four most famous strategies for beat rate assessment.

1.   Because precise IBI evaluation is frequently dangerous, iPPG seldom uses this approach because it is the most quick way to measure beat rate. IBI has to do with the heart's rhythm. Inter beat interval, or IBI, is often defined for iPPG as the time elapsed between successive systolic pinnacles, with some kind of top identification serving as the criterion. We used cubic spline addition to increase the iPPG signal's frequency from 50 to 250 Hz for precise IBI evaluation.

2.   Another methodology is to evaluate normal heartbeat rate as recurrence comparing to proximal scleroderma (PSD), in which PSD is processed over N focuses where one appraisal normal heart rate esteem after some time stretch t = N FSR, here FSR is the inspecting pace of iPPG signal. PSD is typically assessed via (DFT) Discrete Fourier Change or via (AR) autoregressive demonstrating.

3.   (CWT) Continuous Wavelet Transform gives a propitious option in contrast to AR demonstrating and DFT. We have carried out CWT utilizing MATLAB work cwtf. We have picked these scales to have an adequately decent inclusion of human pulse data transmission (0.65–4Hz). Component 20.03125 gives 32 scales for each octave. Because the heart rate gauges for DFT and AR only indicate the usual rate of heartbeat, we used a window size of τ=20.48 s to arrive at the midpoint for IBI and CWT.

4.   Plane-orthogonal to skin (POS) improves CHROM, a CHROM method that uses fluctuation in color intensity as an instance of ppg-induced color variation. In here RGB signals are projected on a plane symmetrical to a standardized complexion in a standardized RGB space, after which it is joined with the subsequent signs into a solitary sign comprising the pulsatile data. Owing to which we present extra sign refinement ventures for exact pinnacle location to additionally further develop HRV and HR investigation.

Chapter 4: Implementation of Algorithm

4.1 Experimental Setup

In the arrangement for video recording the subject was approached to sit on a seat before camera to limit any development relics. The recorded video from two picture catch instruments for this review, worked in camera in iPhone 7 (Apple inc, USA) what's more DSLR Cannon iT3 advanced camera. The camera was mounted on tri-unit and recorded the districts around face of the subject with average surrounding sunlight as wellspring of enlightenment alongside glaring light. These recordings were recorded with 24-bit RGB (3 channels and 8 pieces each) at 60 casings each second (fps) with a goal of 1280x720. The recordings were saved in .mov design. These recordings were taken with the subjects inside 1 meter of skin surface. The investigations were directed inside and open air with satisfactory daylight as the main wellspring of brightening. The subjects were situated to limit development a way off of 0.5 meters from the portable camera utilized for recording. During the shoot the subjects were approached to limit development and gaze straight into the recording camera. A contact-based estimation was utilized for approval of estimation utilizing picture photograph plethysmography (IPPG).

4.2 Signal Extraction

The recorded video was stacked into MATLAB (The Math Works, Inc.) work area, and manual choice of ROI was done to restrict the estimation locale inside the face video. The red (R), green (G) and blue (B) channels of the ROI district were isolated and spatially found the middle value of to yield time series signals R(t), G(t) and B(t) separately. Normal upsides of pixels inside ROI is utilized to work on the SNR and apply Fourier examination to appraise the recurrence range substance of the time differing signal.

Comparatively standardized bends for red (R(t)) and blue (B(t)) channels, where μ and σ are the mean and standard deviation of individual channels. These standardized follows had zero-mean and unit fluctuation as displayed in Fig.4.1.

For beat adequacy planning each edge of the picture was partitioned into coarse lattice of square boxes with a client defined block size. Spatial averaging in such coarse matrix

works on the SNR of the sign. It shows the power range upsides of each square on a basic level rate recurrence to imagine the 'power guide' and attempt to examine the impacts of various square size.

4.3 Heart Rate Estimation Algorithm

The time series signal is isolated into 30s moving window with 29s cross-over. The range investigation of the relative multitude of windows is utilized for the assessment of pulse.
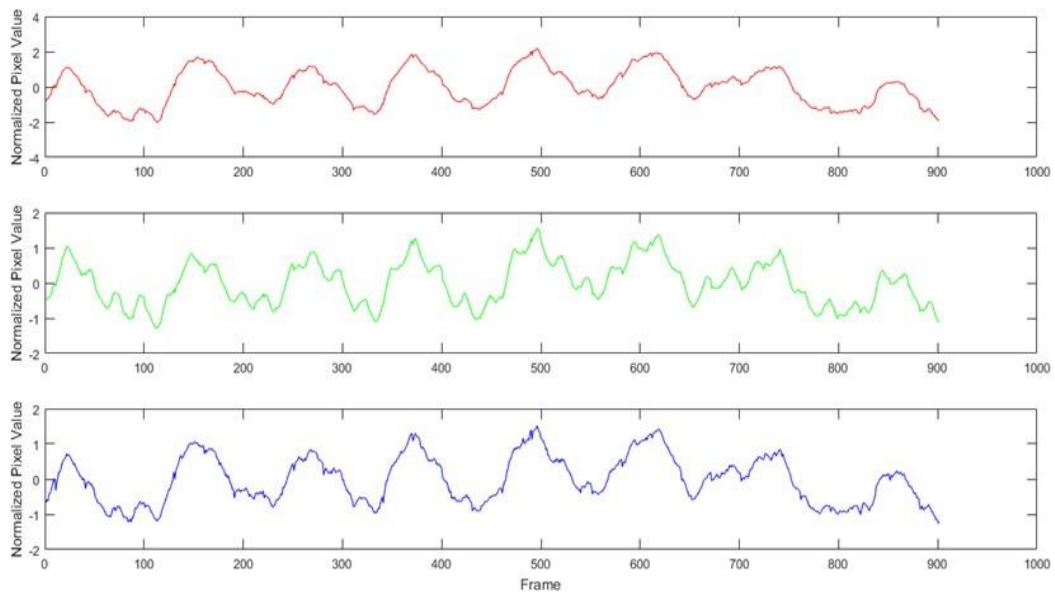

Figure 4.1: Red, Green and Blue Channel indicating Normalized pixel values used to estimate heart rate [25]

The range of the separated green channel shows clear pike at the pulse recurrence. As displayed in Fig.4.2, probably the most noteworthy pinnacle likewise relates to likely recurrence range for heart cycle, where 1.2 Hz = 72 thumps each moment (bpm). Pulse (HR) is defined as the quantity of beats each moment (bpm) and is regularly in the scope of 40 to 240 bpm. HR is generally isolated into two methods of activity, (I) first when the body is very still without an actual strain the pulse is in the scope of 60-100 bpm and (ii) other working reach is the point at which the body is feeling the squeeze with the pulse in scope of 60 bpm to most extreme conceivable HR, which is reliant upon age, sex and physical fitness, which by and large lies in the scope of 180 +/ - 20 bmp.

The recordings were recorded with subjects under great lighting condition and resting position to stay away from any outer curios. This simplifies the pre-handling required for the video arrangement. The ROI was chosen physically and the normal

upsides of red, green and blue channels across outlines. Noticed regulation with pulse in the green channel significantly contrasted with the red or blue channel, as clarified by the retention range of haemoglobin. The spatial averaging approach was successful and showed promising outcomes. The pulse was assessed from range of time-differing signal as displayed Fig.4.3. The HR was acquired as the most often happening HR (method) of the HR estimation from various windows.

These techniques are found to sufficient, vigorous and productive for handling of recorded apparent video. Research [36], recommends the utilization of Independent Component Analysis (ICA) in separating photoplethysmography (PPG) pulse data and back this with test results. ICA, in this study is applied to flag removed from a video section utilizing identification recordings. The further review, impact of applying ICA-JADE [8, 41] for various ROI with differing outline rates and window size. This empowers to assess likely necessities for solid pulse estimation specifically the effect of video boundaries and their impact on pulse assessment.
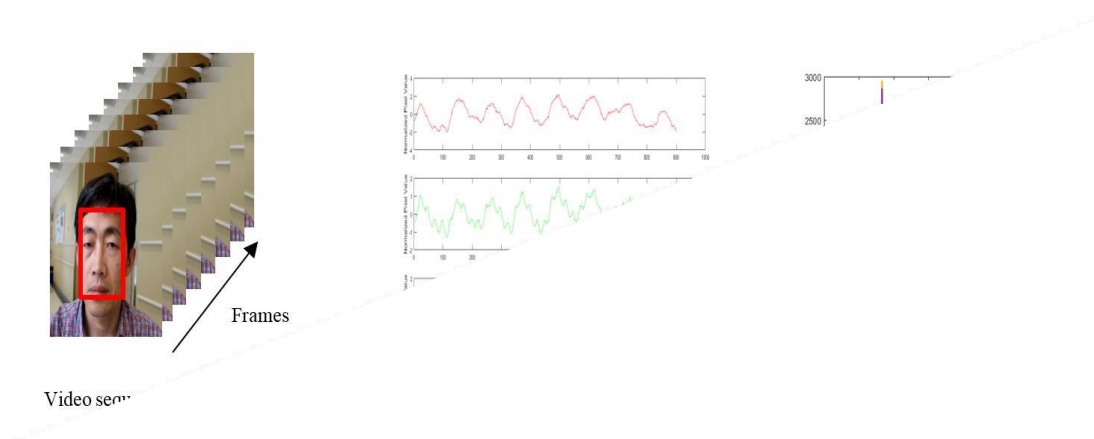

Figure 4.3: Heart rate frequency Spectrum within (0.75,4) Hz frequency range

4.3.1 Independent Component Analysis

The PPG sign of interest is the cardiovascular heartbeat wave that proliferates through body. The progressions in blood stream and volumetric changes in veins during such cardiovascular cycles alter the way of occurrence encompassing light. The recorded video contains a combination of hidden PPG signal alongside different wellsprings of vacillation that incorporate antiques because of movement or change in surrounding lighting conditions. These noticed signs record a combination of unique PPG signal with various commitments to red, green and blue shading sensors. Ordinary ICA is a unique instance of more extensive idea of visually impaired source partition (BSS), which expects a straight change of unique source signals. ICA accepts that number of recoverable signs can't surpass the quantity of perceptions and can be communicated as:

$$x(t) = M.s(t) \tag{4.1}$$

where the vectors $x(t) = [R(t)\ G(t)\ B(t)]\ T$, $s(t) = [s1(t)\ s2(t)\ s3(t)]$ and the 3x3 lattice M holds blend coefficients in its square shape. The ICA attempts to find the W grid that isolates the sign, it is identical to converse of blending framework M, given $x(t)$.

$$s(t) = Wx(t) \tag{4.3}$$

$$[s\ (1);\ s\ (2);\ s\ (3)] = M^{-1}:\ [x\ (1);\ x\ (2);\ x\ (3)] \tag{4.4}$$

$s(t)$ is an estimate of the underlying physical signals, where $x(t)$ is the vector of observed signals. In ICA, W is the matrix that optimizes a statistical measure of the independence of the components of s. (t).

The fundamental standard in view of focal breaking point hypothesis, which recommends an amount of autonomous arbitrary factors is more gaussian than the first factor. In this manner W attempts to augment the non-gaussianity of each source signal. The most broadly utilized measures incorporate non gaussianity of the factors, a property that (by focal breaking point hypothesis) infers freedom. This can be accomplished through iterative arrangements that attempt to boost or limit cost works that action approximations of non gaussianity through kurtosis [41], negentropy [41] or shared data [41].

As referenced above, various iterative calculations can be utilized for ICA relying upon the models for measurable freedom. FastICA [16], InfoMax [6] and Joint Approximation Diagonalization of Eigenmatrices (JADE) [41] are among the couple of generally involved calculations for ICA. Contingent upon the information to be investigated, various calculations are favoured distributions [25, 27, 28] give a correlation of various ICA calculations. This multitude of techniques attempt to rough the demixing grid (W) which is the estimation of the converse of blending network (M). JADE calculation execution in MATLAB [41], in view of its computational benefit of utilizing network calculation including lattice diagonalization like Principal Component Analysis. JADE is most generally utilized for ICA and shows steady and dependable outcomes. It utilizes fourth-request "cumulants" cluster from the information and the subtleties of the calculations can be audited in [41]. It works by giving the first signals as MATLAB column vectors. It then, at that point, investigates the accounts and results the purported W framework, which is utilized to extricate unique sources from perceptions. To sum up the Heart rate assessment calculation is as per the following:

4.4 Pulse Amplitude Mapping

The video recording was stacked into the MATLAB work area. The MATLAB maps the general heartbeat amplitudes in the green channel by jumping the casings into matrices of required square size. The calculations for beat adequacy planning is as per the following:

<u>Algorithm 1: Heat rate Estimation</u>

1: Video object with a goal of 1280x720 pixels, 24-digit RGB shading, and 60 frames per second should be built.

2: Capture a single edge and determine ROI based on the square shape selected by the client.

3: Record the ROI and the green channel's usual substance for N seconds for each casing.

4: (Optional) Apply ICA to appraise the source signals for R, G and B channels

5: Calculate PSD and identify its top in the stretch [0.75 4] Hz for example [40 240] bpm

6: Track the pulse estimation inside 10% variety of past perusing as substantial estimation

7: Calculate the method of pulse assessed from various windows

Pulse amplitude maps (Power maps) inside district of revenue are valuable devices to appraise locales with solid pulse signal and recognize movement antiquities [45]. The skin locales around brow and cheeks show clear difference in power maps for pulse assessment contrasted with the environmental factors.

Chapter 5: Results and Simulation

The video handling and examination of estimation was done in MATLAB. An outline of the pulse assessment is displayed in Fig.5.3. In the event of face video recording chosen the face area as ROI physically, then, at that point, the video was handled as three separate channels red, green and blue. The pixels esteem inside the ROI were arrived at the midpoint of to give perusing of the red, green and blue channels across outlines.

Algorithm 2: Pulse Amplitude Mapping

1: Construct matrix partitioning the video outline into non-covering square locales. The size of these blocks (block Size) is an exchange between sign to noise ration and resolution

2: Average the pixel esteems in each container across edges to create the time series signal, which are subsequently standardized to zero mean and unit standard deviation

3: Record the ROI and the green channel's usual material for N seconds for each casing.

4: (Optional) The R, G, and B channels' source signals can be identified using ICA.

5: For each square ascertain the FFT utilizing the standardized/assessed (G/G') green channel (after ICA).

6: Calculate Power Spectrum Density (PSD) and distinguish its top in the stretch [0.75 4] Hz (for example [45 240] bpm),

7: Track the pulse estimation inside 10% variety of past perusing as legitimate estimation, pulse is the method of pinnacles recognized in various boxes

8: Select the power range esteems at the pulse assessed from various matrices in ROI and refreshed the network esteems to create the power map
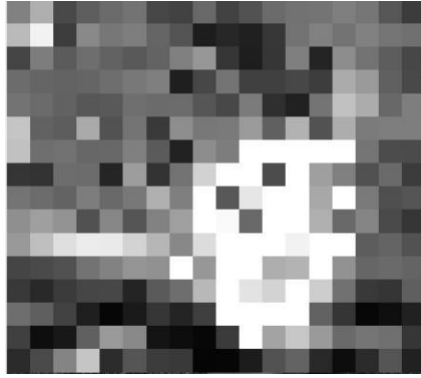
Figure 5.1: Pulse Amplitude Map at Heart rate frequency with 50x50 grid size
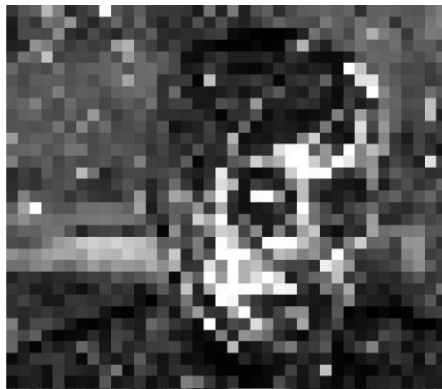
Figure 5.2: Pulse Amplitude Map at Heart rate frequency with 25x25 grid size

Figure 5.3: Pulse Amplitude Map at Heart rate frequency with 10x10 grid size

These red, green and blue follows are standardized to remove the AC signal over the DC. These standardized signs are utilized for FFT investigation. FFT Spectrum investigation was finished utilizing standardized signs utilizing standardized signs over a window width of 30 seconds and 29 seconds cross-over, trailed by top location for Pulse recurrence assessment. To eliminate exceptions because of movement antiquities

any shift in perspective pace of over 10% in one or the other bearing starting with one window then onto the next was viewed as a mistake and elective pinnacles were utilized to identify pulse. Top identification was done inside windows of 0.75 Hz to 4 Hz relating to 45 to 240 bpm.

An instance of assessing pulse from video recording is displayed in Fig.5.4. The assessment of pulse of a subject very still with video recording for 2 minutes span. It additionally shows the 30s window of RGB follows after standardization. Fig.5.4 shows the 30s windows of the RGB follows got by averaging pixel esteems in ROI. Notice PPG signal as an AC regulation over the DC signal. The power range of the green channel after ICA JADE shows a reasonable top at 1.13 Hz demonstrating pulse alongside certain music.

Video sequence   Time/Frame series signal   Frequency Spectrum
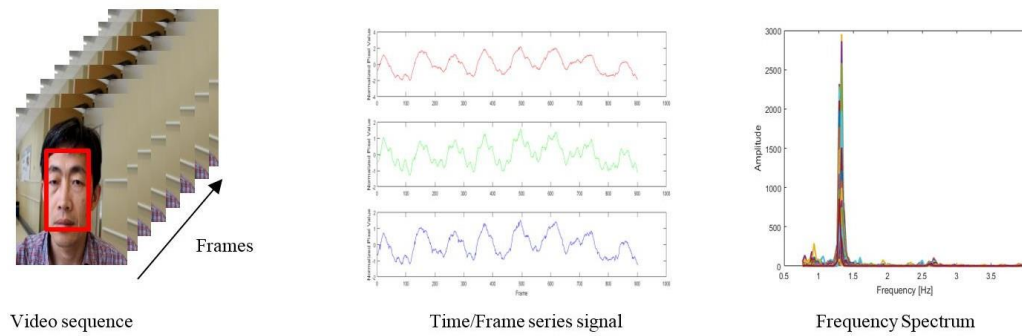
Figure 5.4: Heart rate estimation (a) ROI Selection (b) Time Series signal and (c) Frequency Spectrum

An unmistakable top in the power range showing pulse. To assess the impact of ICA on assessing pulse straightforwardly from the green channel and subsequent to applying ICA-JACE calculation for pulse assessment.

5.1 Heart Rate Measurement from Face Region

In the video loaded into MATLAB, selection of face regions was done manually as shown in Fig.5.5. The face regions used for selection is 60% width and height of the face [36]. We assessed heart rate through RGB video in order to confirm the helpfulness of the (iPPG) imaging Photoplethysmogram signal for beats assessment in individuals.

Quality measurements were also made to describe how the video's heart rate compared to the reference heart rate obtained using a beat oximeter (refPR) in the middle of the beat. Here, for better proficiency we have taken the video of least size 0f 15 secs to guarantee distinctive lighting impacts and better heartbeat rate assessment.
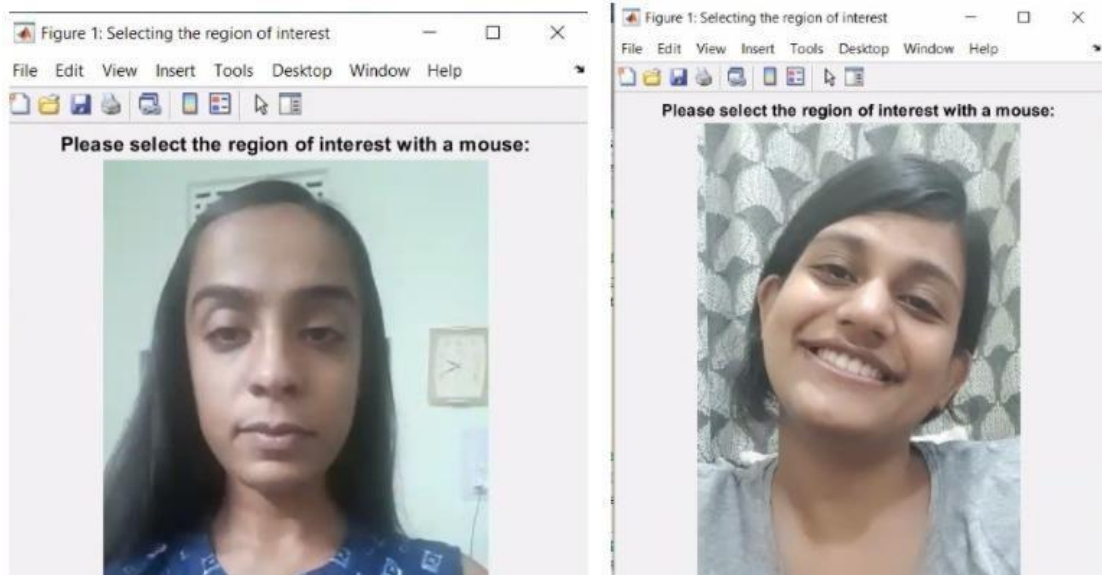

Figure 5.5: ROI Selection for IPPG - Face Region

Subsequent to choosing the Locale of Interest in the initial step, presently the transformation of pictures from the video would be handled. To guarantee greatest proficiency the transformation from RBG happens just for the return for capital invested.
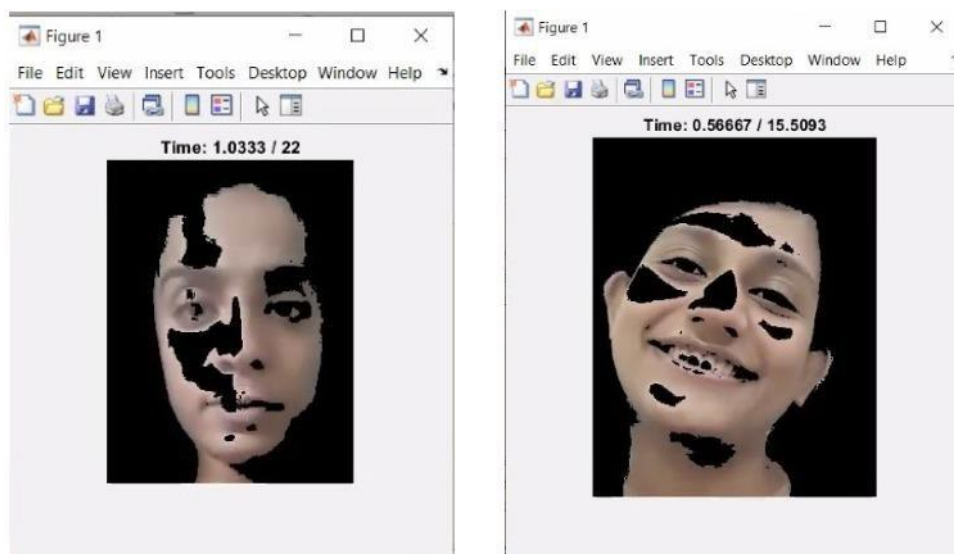
Figure 5.6: RGB conversion of selected ROI

After the change, the pre-processing and post-handling steps are completed on the pictures recuperated from the video. Here, in this paper we have assessed the iPPG from the POS strategy talked about above.
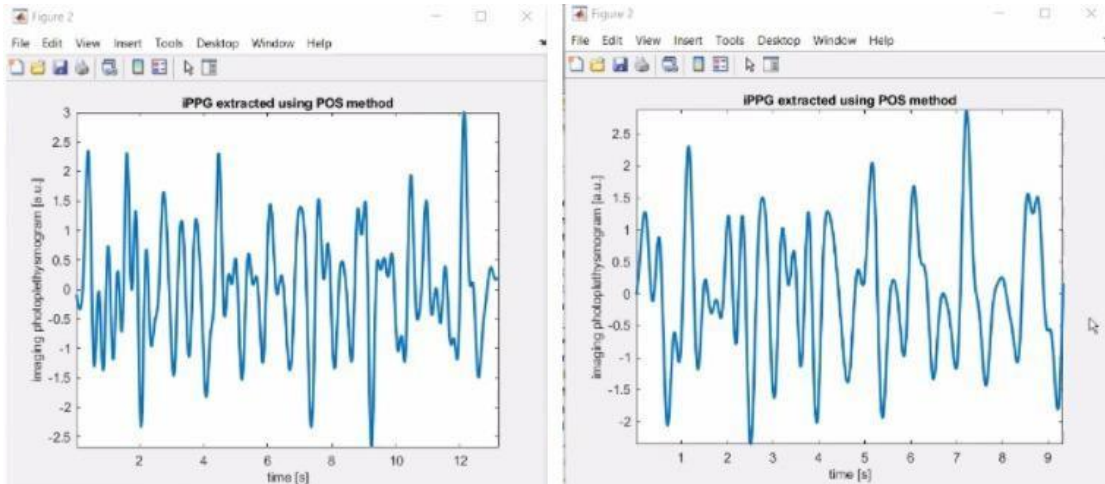
Figure 5.7: iPPG Extraction using POS method

At long last, we have separated the signs and assessed the PPG utilizing Continuous Wavelet Change (CWT).
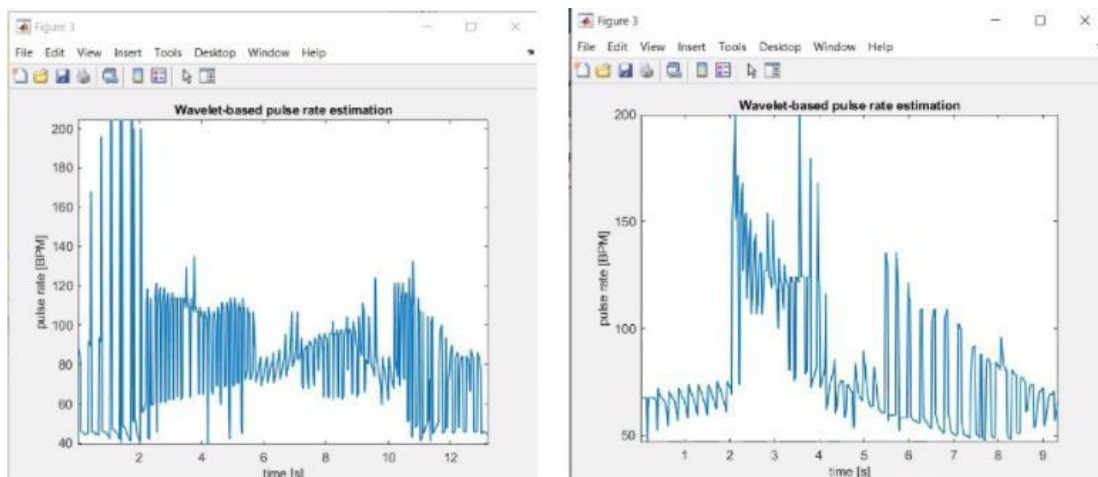
Figure5.8: Wavelet based iPPG extraction

In all circumstances, the best results are achieved for the full face, with skin determination and anomalies eliminated out. The most reduced assessment blunders were accomplished when iPPG extraction was accomplished using POS and beat rate assessment via CWT. Out and out, upsides of value measurements are similar to those revealed during the writing for beat rate assessment via uncompressed video.

We utilize pre and present handling on guarantee the best SNR and gauge beat rate by CWT. CWT provided the best results and measurements compared to the listed methods. This technique is particularly valuable since it permits us to gauge normal as well as transitory heartbeat rate.

Other tried techniques for beat rate assessment had specific downsides. Like, DFT gave subsequently the best outcome as far as assessment mistake and part of effectively assessed ages, yet it had low recurrence goal. Most insignificant and all-round execution was achieved by POS method which was visible in the idea where (iPPG) imaging Photoplethysmogram was eliminated from the DEAP dataset.

Chapter 6: Conclusion

With skin assurance and unique excusal, optimal results are obtained in all situations for the entire face return on the investment given. As far as iPPG extraction and beat rate appraisal go, the largest reduced evaluation errors were found while applying POS and CWT, respectively. Uncompressed video beat rate estimate yields comparable benefits to those found in the composition for beat rate estimation from uncompressed video.

The optimum SNR is ensured and the CWT beat rate is checked using pre- and post-care. CWT provided the most accurate estimates, hence the best outcomes were obtained. As a result of this procedure, we are able to examine the heartbeat rate of an individual who is merely passing over. Other approaches for evaluating beat rates have clearly stated limitations. DFT yielded the highest results in the quantity of appraisal mistakes and part of properly appraised ages, but it had low repeat objectives. DEAP accounts loaded with iPPG were the most insignificant all-around execution, which may be explained by the lack of an iPPG concept in the POS evaluation.

In this thesis, we concentrate on the pulse extraction utilizing versatile camera video of the subject utilizing simply encompassing light. We attempt to approve the estimation technique utilizing beat sufficiency planning. We research the exhibition of the pulse assessment in light of various video boundaries like edge rate, goal, time windows and different lattice sizes for beat adequacy planning. A reasonable sign was separated from manual division of ROI. These techniques can be mechanized through basic face identification/following calculations. The range of video signal shows a few music to base HR recurrence. The ICA calculation as concentrated in [45], shows improvement in pulse assessment particularly for loud announces eliminating lower-recurrence unsettling influences. The noticed exhibition of pulse assessment shows a mean mistake of 2.01 bpm and 5.31 bpm of 95 % limits for blunder estimation (mean 1.96 SD), contrasted with contact-based PPG. Pulsativity planning, from a video with least development shows the cleanest signal. The Pulsativity (beat plentifulness planning) shows great approval for the assessed pulse by showing solid sign in the face locales contrasted with environmental elements particularly for the brow also cheeks. It is helpful for planning locales with solid PPG signal or disposing of areas with less pulsatile signal.

Additionally, a few boundaries apparently had effect on the nature of the obtained throbbing sign. The nature of the PPG signal saw from video is seriously limited by light changes, development antiques and clamour. These concentrates plainly show the chance of assessing pulse from business grade video recording. The tests with outline rate changing from 60 fps to 10 fps, show great consistency, empowering precise assessment of pulse from poor quality video recording. After examination with various ROI determination, the front head districts are viewed as steady site for assessment of pulse. Subsequently, the outcomes show great guarantee in execution of IPPG for pulse checking particularly for mass fever screening as a chance, where minimal expense of establishment and adaptability are significant.

Appendix A: Result Analysis

A.1 Bland-Altman Analysis

The Bland-Altman examination/plot is utilized as graphical strategy to think about two estimation procedures. This incorporates plots between contrast of two estimations against the mean of the two estimations. These plots are utilized to recognize the mean contrast and 95% cut-off points under the supposition of gaussian appropriation for example mean + - 1.96 SD of the distinction. These plots can be utilized to gauge any methodical predisposition between the size of the estimation and blunder. The fundamental perception in such plots is the mean + - 1.96 SD, assuming the upsides of these cut-off points is clinically satisfactory the two techniques can be utilized reciprocally.

A.2 Recall Graphs

We assess review charts to have quantitative assessment of enrolment precision. We measure the Euclidean distance between the milestone in the changed moving places and comparing tourist spots in reference picture. We figure review on all the milestone sets of districts as metric utilized in [21]. The genuine positive rate, is defined as the negligible portion of genuine positive correspondences, which is defined as when two comparing sets fall inside a given precision limit as far as pairwise distance.

Appendix B

```matlab
% iPPG extraction
fontSize = 10;
fontType = 'Arial';
lineWidth = 2;


%% Step 1: extracting raw color signals from the video
videoSettings = struct('manualROIselection', true, ...
                'isSTDmaskingOn', true, ...
                'stdCoef', 1.5, ...
                'isHSVmaskingOn', true, ...
                'hsvMin', [0.00, 0.09, 0.34], ...
                'hsvMax', [0.13, 0.52, 1.00]);


%Please set a correct path to the video file:
video_path = 'C:\Users\Shivangi\OneDrive\Desktop\MTech\MATLAB\pulse rate
estimation\Imaging-photoplethysmogram-extraction-pulse-rate-estimation-
master\video5.avi';
rawColorSignal = extract_color_channels_from_video(video_path, videoSettings);


%% Steps 2-4: compute and process imaging photoplethysmogramm (iPPG)
VIDEO_SR = 50.0; % video sampling rate
if (VIDEO_SR > 50)
   FFT_WINDOW_SIZE = 2048;
elseif (VIDEO_SR > 25)
   FFT_WINDOW_SIZE = 1024;
else
   FFT_WINDOW_SIZE = 512;
end
ippgSettings = struct('PROCESSING', struct('SPA_DETRENDING', 2^0, ...
                        'PRE_MA_FILTER', 2^1, ...
                        'PRE_BANDPASS_FILTER', 2^2, ...
```

```matlab
                        'POST_MA_FILTER', 2^3, ...
                        'POST_BANDPASS_FILTER', 2^4, ...
                        'OUTLIERS_SUPPRESSION', 2^5, ...
                        'POST_WAVELET_FILTER', 2^6, ...
                        'ADAPTIVE_BAND_FILTER', 2^7), ...
              'EXTRACTION', struct('GREEN', 1, ...
                        'ICA', 2, ...
                        'CHROM', 3, ...
                        'POS', 4, ...
                        'G_MINUS_R', 5, ...
                        'AGRD', 6), ...
        'minFreq', 0.65, ...
        'maxFreq', 4.00,...
        'samplingRate', VIDEO_SR, ...
        'processing', 0, ...
        'extractionMethod', 0, ...
        'maFilterLength', 5, ...
        'bandpassFilterOrder', 127, ...
        'stdWindowLength', fix(VIDEO_SR), ...
        'waveletFilterWidth', [2, 5], ...
        'waveletFilterAveragingLength', 20*VIDEO_SR, ...
        'fftWindow', FFT_WINDOW_SIZE, ...
        'fftShiftSize', ceil(FFT_WINDOW_SIZE/2));


ippgSettings.processing = ippgSettings.PROCESSING.OUTLIERS_SUPPRESSION + ...
              ippgSettings.PROCESSING.POST_BANDPASS_FILTER;
ippgSettings.extractionMethod = ippgSettings.EXTRACTION.POS;
iPPG = compute_ippg(rawColorSignal, ippgSettings);


xValues = (1:length(iPPG))/ippgSettings.samplingRate;


figure
set( axes,'fontsize', fontSize,  'FontName', fontType);%'FontName', 'Times');
plot(xValues, iPPG, 'LineWidth', lineWidth)
```

```matlab
set( gca, 'fontsize', fontSize, 'FontName', fontType);
xlabel( ' time [s] ', 'fontsize', fontSize, 'FontName', fontType);
ylabel( ' imaging photoplethysmogram [a.u.] ', 'fontsize', fontSize, 'FontName', fontType);
title('iPPG extracted using POS method', 'fontsize', fontSize, 'FontName',fontType)
axis tight


%% Steps 5: pulse rate estimation
% pulse rate estimation using Discrete Fourier Transform:
[hrEstimatedFFT, spectrum] = DFT_pulse_rate_estimate(iPPG, ippgSettings);
% pulse rate estimation using wavelet transform:
[hrEstimatedWavelet, hrMomentaryWavelet] = wavelet_pulse_rate_estimate(iPPG,
ippgSettings);


xValues = (1:length(hrMomentaryWavelet))/ippgSettings.samplingRate;
figure
set( axes,'fontsize', fontSize,  'FontName', fontType);%'FontName', 'Times');
plot(xValues, hrMomentaryWavelet, 'LineWidth', 1)
set( gca, 'fontsize', fontSize, 'FontName', fontType);
xlabel( ' time [s] ', 'fontsize', fontSize, 'FontName', fontType);
ylabel( ' pulse rate [BPM] ', 'fontsize', fontSize, 'FontName', fontType);
title('Wavelet-based pulse rate estimation', 'fontsize', fontSize, 'FontName',fontType)
axis tight
```

%DFT PULSE RATE ESTIMATION

```matlab
function [pulseRate, spectrum] = DFT_pulse_rate_estimate(ippgSignal, ippgSettings)
minHeartFreq = floor(1 + ...
ippgSettings.minFreq*ippgSettings.fftWindow/ippgSettings.samplingRate);
maxHeartFreq = floor(1 + ...
ippgSettings.maxFreq*ippgSettings.fftWindow/ippgSettings.samplingRate);

 w = hamming(ippgSettings.fftWindow)';
 dataLength = length(ippgSignal);
 startPos = 1:ippgSettings.fftShiftSize:(dataLength-ippgSettings.fftWindow+1);
 nWin = length(startPos);
 heartFreqIndex = zeros(1, nWin);
 spectrum = zeros(maxHeartFreq - minHeartFreq + 1, nWin);

 for iWin = 1:nWin
   ppgWindowed = ippgSignal(startPos(iWin):startPos(iWin)+ippgSettings.fftWindow-1).*w;
   ppgFFT = fft(ppgWindowed, [], 2);
   ppgSpectrum2side = abs(ppgFFT/ippgSettings.fftWindow);
   spectrum(:, iWin) = ppgSpectrum2side(minHeartFreq:maxHeartFreq); %take only values in heart rate bandwidth
   %find the maximal frequency (presumably, corresponding to ppg)
   [~, heartFreqIndex(iWin)] = max(spectrum(:, iWin));
 end
 spectrum = bsxfun(@rdivide, spectrum, sum(spectrum));
 % heartFreqIndex + minHeartFreq - 1 is the index of maximal frequency
 % since index = 1 corresponds to frequency 0 Hz (DC), we need to deduce 1:
 pulseRate = (60*ippgSettings.samplingRate/ippgSettings.fftWindow)*(heartFreqIndex + minHeartFreq - 2);
end
```

%WAVELET PULSE RATE ESTIMATION

```matlab
function [pulseRate, instantPulseRate] = wavelet_pulse_rate_estimate(ippgSignal,
ippgSettings)
 % wavelet transform
 sig = struct('val',ippgSignal, 'period', 1/ippgSettings.samplingRate);
 waveName = {'morl', []};
 sca = wavelet_init_scales(ippgSettings);
 cwtstruct = cwtft(sig, 'wavelet', waveName, 'scales', sca) ;

    % determine limits within those we search for pulse rate
 MorletFourierFactor = 4*pi/(6+sqrt(2+6^2));
 freq = 1./(cwtstruct.scales.*MorletFourierFactor);
 firstScaleIndex = find(freq < ippgSettings.maxFreq, 1, 'first');
 lastScaleIndex = find(freq < ippgSettings.minFreq, 1, 'first');

 % compute power spectrum
 energyProfile = abs(real((cwtstruct.cfs.^2)));

 % to estimate momentary pulse rate, for every moment of time
 % we compute frequencies having maximal power within pulse rate limits
 [~, instantPulseRateScales] = max(energyProfile(firstScaleIndex:lastScaleIndex, :));
 instantPulseRate = 60*freq(firstScaleIndex + instantPulseRateScales - 1);

 % compute average pulse rates by computing moving average of spectrum
 % and considering only time points with distance ippgSettings.fftShiftSize
 w = ones(1, ippgSettings.fftWindow) ./ ippgSettings.fftWindow;
 energyProfileMean = conv2(energyProfile, w, 'valid');
 [~, maxPos] = size(energyProfileMean);
 pos = 1:ippgSettings.fftShiftSize:maxPos;
 [~, pulseRateScales] = max(energyProfileMean(firstScaleIndex:lastScaleIndex, pos));
 pulseRate = 60*freq(firstScaleIndex + pulseRateScales - 1);
end
```

%EXTRACT COLOUR CHANNELS FROM VIDEO

```matlab
function rawColorSignal = extract_color_channels_from_video(filename, videoSettings)
videoObject = VideoReader(filename);


% filling the missing fields of the settings stucture
if (~isfield(videoSettings,'cascadeROIselection'))
    videoSettings.cascadeROIselection = false;
end
if (~isfield(videoSettings,'manualROIselection'))
    videoSettings.manualROIselection = false;
end


nFrame = ceil(videoObject.FrameRate*videoObject.Duration);


if (hasFrame(videoObject)) % set initial ROI
    currentFrame = readFrame(videoObject);
    if (videoSettings.manualROIselection)
        % manual selection of ROI rectangle in the first frame
        rectROI = loc_manual_ROI_selection(currentFrame);
    else
        % ROI rectangle covers the whole frame
        rectROI = [1,1,videoObject.Width, videoObject.Height];
    end
    widthROI = rectROI(3);
    heightROI = rectROI(4);
    rawColorSignal = zeros(3, nFrame); % preallocate array
else
    error('Video processing failed: no frames are available!');
end


if (videoSettings.cascadeROIselection) % initialize face detector
    faceExpectedRect = [1, 1, widthROI, heightROI];
end
```

```matlab
% process all individual frames
for iFrame = 1:nFrame
    % disp(strcat(['Processing frame:', ' ', num2str(iFrame)]))
    if (iFrame > 1) %the first frame is already loaded
        if (~hasFrame(videoObject))
            break
        end
        currentFrame = readFrame(videoObject);
    end
    croppedImage = loc_crop_image(currentFrame, rectROI); % crop initial ROI rectangle


    if (videoSettings.cascadeROIselection) % detect face if necessary
        faceRect = loc_cascade_ROI_selection(croppedImage, faceExpectedRect);
        facialImage = loc_crop_image(croppedImage, faceRect);
    else
        facialImage = croppedImage;
    end
    currentROI = loc_ROI_refinement(facialImage, videoSettings); % filter out bad pixels


    % check whether ROI due to face detection didn't become less than 4 pixels
    if (videoSettings.cascadeROIselection)
        if (sum(sum(currentROI)) < 4)
            facialImage = loc_crop_image(croppedImage, faceExpectedRect);
            currentROI = loc_ROI_refinement(facialImage, videoSettings);
            faceRect = faceExpectedRect;
        else
            faceExpectedRect = faceRect;
        end
    end


    % show the video frames
    maskedImage = facialImage;
    for iChannel = 1:3
```

```matlab
        colorChannel = maskedImage(:,:,iChannel);
        colorChannel(~currentROI) = 1;
        maskedImage(:,:,iChannel) = colorChannel;
    end
    imshow(maskedImage);
    title(['Time: ' num2str(iFrame/videoObject.FrameRate) ' / '
num2str(videoObject.Duration)]);
    drawnow update

    % compute the average color values over the ROI
    for iChannel = 1:3
        colorChannel = facialImage(:,:,iChannel);
        rawColorSignal(iChannel,iFrame) = mean(mean(colorChannel(currentROI)));
    end
end
end


% manual selection of ROI rectangle in the first frame
function rectROI = loc_manual_ROI_selection(currentFrame)
figureHandle = figure('Name', 'Selecting the region of interest');
imshow(currentFrame);
title('Please select the region of interest with a mouse:');
h = imrect;
if isempty(h)
    warning('Video processing interrupted by user');
    return;
end
h.Deletable = false;
addNewPositionCallback(h,@(p) title([mat2str(round(p),3), ', double click on ROI to
continue...']));
fcn = makeConstrainToRectFcn('imrect',get(gca,'XLim'),get(gca,'YLim'));
setPositionConstraintFcn(h,fcn);
title([mat2str(round(getPosition(h)),3), ', double click on ROI to continue...']);
rectROI = round(wait(h));
```

```matlab
if isempty(rectROI)
    warning('Video processing interrupted by user');
    return;
end
close(figureHandle);
end


% localising the face using Viola-Jones algorithm
function faceRect = loc_cascade_ROI_selection(currentFrame, faceExpectedRect)

faceDetector = vision.CascadeObjectDetector;
[~, frameWidth, ~] = size(currentFrame);

faceRect = faceExpectedRect; % if we do not find a new face, simply use the last location

faces = step(faceDetector, currentFrame);
[nFace, ~] = size(faces);

if (nFace > 0) % faces found
    % center of faceRect cannot move between successive frames on more than a half of the
faceRect diagonal
    maxDist = sqrt(faceExpectedRect(3)^2 + faceExpectedRect(4)^2)/2;
    % area cannot decrease more than twice
    minArea = faceExpectedRect(3)*faceExpectedRect(4)/2;
    if (faceExpectedRect(3) >= 0.95*frameWidth) % if expected face is too large
        minArea = 9;  % consider it incorrect and set facial area threshold to a small const
    end
    expectedCenter = [faceExpectedRect(1) + 0.5*faceExpectedRect(3), ...
        faceExpectedRect(2) + 0.5*faceExpectedRect(4)];

    % check all detected faces to find the one
    for iFace = 1:nFace
        faceCenter = [faces(iFace, 1) + 0.5*faces(iFace, 3), ...
            faces(iFace, 2) + 0.5*faces(iFace, 4)];
```

```matlab
            currDist = norm(faceCenter - expectedCenter);
            if ((currDist < maxDist) && (faces(iFace, 3)*faces(iFace, 4) > minArea))
                maxDist = currDist;
                faceRect = faces(iFace, :);
                % reduce the width of the face as it is done by Picard group
                faceRect(1) = faceRect(1) + 0.1*faceRect(3);
                faceRect(3) = 0.8*faceRect(3);
            end
        end
    end
end
% function for filtering bad pixels (non-skin or corrupted with artefacts)
function currentROI = loc_ROI_refinement(croppedImage, videoSettings)
    [heightROI,widthROI,~] = size(croppedImage);
    currentROI = ones(heightROI,widthROI);
    % HSV filtering: pixels with hue, saturation or value
    % outside of the specified range are discarded
    if (videoSettings.isHSVmaskingOn && (length(videoSettings.hsvMin) == 3) &&
(length(videoSettings.hsvMax) == 3))
        hsvFrame = rgb2hsv(croppedImage);
        for iChannel = 1:3
            hsvMask = roicolor(hsvFrame(:,:,iChannel), videoSettings.hsvMin(iChannel),
videoSettings.hsvMax(iChannel));
            currentROI = currentROI & hsvMask;
        end
    end

    % std thresholding: pixels with color channels too far from the mean
    % are discarded
    if (videoSettings.isSTDmaskingOn)
        stdMask = currentROI;
        for iChannel = 1:3
            colorChannel = croppedImage(:,:,iChannel);
            channelMean = mean(mean(colorChannel(currentROI)));
```

```matlab
        channelStd  = std2(colorChannel(currentROI));
        minChannelValue = channelMean - videoSettings.stdCoef*channelStd;
        maxChannelValue = channelMean + videoSettings.stdCoef*channelStd;
        % we do not modify here currentROI since we need it to compute std corretly
        stdMask = stdMask & roicolor(colorChannel, minChannelValue, maxChannelValue);
    end
    currentROI = currentROI & stdMask;
  end
end



% wrapper for cropping the image
function croppedImage = loc_crop_image(image, rect)
  croppedImage = imcrop(image, [rect(1:2), rect(3:4)-1]);
end
```

%JADE ALGORITHM

```
verbose = 0;    % Set to 0 for quiet operation


% Finding the number of sources
[n,T]  = size(X);
if nargin==1, m=n ; end;    % Number of sources defaults to # of sensors
if m>n ,   fprintf('jade -> Do not ask more sources than sensors here!!!\n'), return,end
if verbose, fprintf('jade -> Looking for %d sources\n',m); end ;


% Mean removal
if verbose, fprintf('jade -> Removing the mean value\n'); end
X  = X - mean(X')' * ones(1,T);


%%% whitening & projection onto signal subspace
if verbose, fprintf('jade -> Whitening the data\n'); end


[U,D]    = eig((X*X')/T) ; %% An eigen basis for the sample covariance matrix
[Ds,k]   = sort(diag(D)) ; %% Sort by increasing variance
PCs      = n:-1:n-m+1    ; %% The m most significant princip. comp. by decreasing variance


%% -- PCA ------------------------------------
B       = U(:,k(PCs))'    ; % At this stage, B does the PCA on m components


%% -- Scaling ---------------------------------
scales   = sqrt(Ds(PCs)) ; % The scales of the principal components .
B       = diag(1./scales)*B  ; % Now, B does PCA followed by a rescaling = sphering


%% -- Sphering ---------------------------------
X       = B*X; %% We have done the easy part: B is a whitening matrix and X is white.


clear U D Ds k PCs scales ;
```

```matlab
%%% Estimation of the cumulant matrices.
if verbose, fprintf('jade -> Estimating cumulant matrices\n'); end


%% Reshaping of the data, hoping to speed up things a little bit...
X = X';
 dimsymm     = (m*(m+1))/2; % Dim. of the space of real symm matrices
nbcm       = dimsymm ;    % number of cumulant matrices
CM     = zeros(m,m*nbcm); % Storage for cumulant matrices
R     = eye(m);  %%
Qij       = zeros(m); % Temp for a cum. matrix
Xim     = zeros(m,1);  % Temp
Xijm       = zeros(m,1);   % Temp
Uns     = ones(1,m);    % for convenience

Range     = 1:m ; % will index the columns of CM where to store the cumulant matrices.


for im = 1:m
  Xim = X(:,im) ;
  Xijm= Xim.*Xim ;
  %% Note to myself: the -R on next line can be removed: it does not affect
  %% the joint diagonalization criterion
  Qij         = ((Xijm(:,Uns).*X)' * X)/T - R - 2 * R(:,im)*R(:,im)' ;
  CM(:,Range)  = Qij ;
  Range        = Range + m ;
  for jm = 1:im-1
    Xijm       = Xim.*X(:,jm) ;
    Qij         = sqrt(2) *(((Xijm(:,Uns).*X)' * X)/T - R(:,im)*R(:,jm)' - R(:,jm)*R(:,im)') ;
    CM(:,Range) = Qij ;
    Range       = Range + m ;
  end ;
end;
```

```matlab
% BLAND ALTMAN ALGORITHM
function [means, diffs, meanDiff, confInterval, linRegressCoef] = ...
bland_altman_plot(estimate1, estimate2, sessionIndex)
  colorList = [0.0, 0.0, 0.6; ...
            0.6, 0.5, 1.0; ...
            0.7, 0.4, 0.2; ...
            1.0, 0.8, 0.5; ...

            0.9, 0.0, 0.0; ...
            0.6, 0.1, 0.4; ...
            1.0, 0.6, 0.8; ...

            0.0, 0.9, 0.7; ...

            0.8, 1.0, 0.2; ...
            0.5, 1.0, 0.3; ...
            0.1, 1.0, 0.7; ...
            0.0, 1.0, 0.8; ...
            0.2, 0.6, 0.6; ...
            0.2, 1.0, 1.0; ...
            0.4, 1.0, 1.0; ...
            0.6, 0.9, 0.9; ...
            1.0, 0.2, 0.5; ...
            0.7, 1.0, 1.0];

  if nargin==2
    sessionIndex = 1;
  end

  means = mean([estimate1;estimate2]);
  diffs = estimate1 - estimate2;

  % compute linear regression coefficients
```

```matlab
  mdl = fitlm(means, diffs)
  linRegressCoef = polyfit(means, diffs, 1);


  meanDiff = mean(diffs);
  sdDiff = std(diffs);
  confInterval = [meanDiff + 1.96*sdDiff, meanDiff - 1.96*sdDiff]; % 95% confidence
interval


  minX = min(means) - 2;
  maxX = max(means) + 2;
  minY = min(min(diffs) - 2, confInterval(2) - 3);
  maxY = max(max(diffs) + 2, confInterval(2) + 3);


  % plot results
  hold on
  nColor = max(unique(sessionIndex));
  for iColor = 1:nColor
    index = (sessionIndex == iColor);
    plot(means(index), diffs(index), 'o', 'markersize', 4, 'Color', colorList(iColor, :));
  end


  % plot mean and confidence interval
  plot([minX maxX], [meanDiff meanDiff], 'k-');
  plot([minX maxX], [confInterval(1) confInterval(1)],'k--');
  plot([minX maxX], [confInterval(2) confInterval(2)],'k--');
% plot the regression line
  plot([minX maxX], [minX maxX]*linRegressCoef(1)+linRegressCoef(2),'b:', 'linewidth',
1.5);
  hold off
  axis ( [minX, maxX, minY - 1, maxY + 1 + 0.15*(maxY - minY)] );
% axis ( [minX, maxX, -16.5, 28.5] );
% axis ( [minX, maxX, -35.5, 34.5] );
end
```

References

[1] IEC 80601-2-59: MEDICAL ELECTRICAL EQUIPMENT - PART 2-59: PARTICULAR REQUIREMENTS FOR THE BASIC SAFETY AND ESSENTIAL PERFORMANCE OF SCREENING THERMOGRAPHS FOR HUMAN FEBRILE TEMPERATURE SCREENING.

[2] WHO | Assessment of risk associated with inuenza A(H5N8) virus. WHO, 2017.

[3] Andriy Myronenko. Medical Image Registration Toolbox - Andriy Myronenko.

[4] Akshay Asthana, Stefanos Zafeiriou, Shiyang Cheng, and Maja Pantic. Robust Discriminative Response Map Fitting with Constrained Local Models.

[5] Fr_ed_eric Bousefsaf, Choubeila Maaoui, and Alain Pruski. Remote detection of mental workload changes using cardiac parameters assessed with a low-cost webcam. Computers in Biology and Medicine, 53(C):154{163, oct 2014.

[6] Coni~nunicated By, John Platt, Simon Haykin, Anthony J Bell, and Terrence J Sejnowski. An Information-Maximization Approach to Blind Separation and Blind Deconvolution.

[7] Lung-Sang Chan, Giselle T. Y. Cheung, Ian J. Lauder, and Cyrus R. Kumana. Screening for Fever by Remote-sensing Infrared Thermographic Camera. Journal of Travel Medicine, 11(5):273{279, mar 2006.

[8] Ke-Lin Du and M. N. S. Swamy. Independent Component Analysis. In Neural Networks and Statistical Learning, pages 419{450. Springer London, London, 2014.

[9] C. Y. N. Dwith, Pejhman Ghassemi, Joshua Pfefer, Jon Casamento, and Quanzeng Wang. Multi-modality image registration for e_ective thermographic fever screening. page 100570S. International Society for Optics and Photonics, feb 2017.

[10] Bernd Fischer and Jan Modersitzki. A uni_ed approach to fast image registration and a new curvature-based registration technique. Linear Algebra and its Applications, 380:107{124, mar 2004.

[11] Xuejun Gu, Hubert Pan, Yun Liang, Richard Castillo, Deshan Yang, Dongju Choi, Edward Castillo, Amitava Majumdar, Thomas Guerrero, and Steve B Jiang. Implementation and evaluation of various demon's deformable image registration algorithms on a GPU. Physics in Medicine and Biology, 55(1):207{219, jan 2010.

[12] Alastair D Hay, Tim J Peters, Andrew Wilson, and Tom Fahey. The use of infrared thermometry for the detection of fever. British Journal of General Practice, 54(503), 2004.

[13] Derek L. G. Hill, David J. Hawkes, Neil A. Harrison, and Cli_ F. Ru_. A strategy for automated multimodality image registration incorporating anatomical knowledge and imager characteristics. In Information Processing in Medical Imaging, pages 182{196. Springer-Verlag, Berlin/Heidelberg, 1993.

[14] Berthold K P Horn and Brian G Schunck. Determining Optical Flow.

[15] Kenneth Humphreys, Tomas Ward, and Charles Markham. Noncontact simultaneous dual wavelength photoplethysmography: A further step toward noncontact pulse oximetry. 2007.

[16] Aapo Hyv• arinen, Aapo Hyv• arinen, and Erkki Oja. A Fast Fixed -Point Algorithm for Independent Component Analysis. NEURAL COMPUTATION, 9:1483|-1492, 1997.

[17] Jin Jin Fei and I. Pavlidis. Thermistor at a Distance: Unobtrusive Measurement of Breathing. IEEE Transactions on Biomedical Engineering, 57(4):988{998, apr 2010.

[18] E Kee and E Ng. Fever Mass Screening Tool for Infectious Diseases Outbreak. In Medical Infrared Imaging, pages 16{1{16{19. CRC Press, jul 2007.

[19] Thomas M Lehmann, Claudia G• onner, and Klaus Spitzer. Survey: Interpolation Methods in Medical Image Processing. IEEE TRANSACTIONS ON MEDICAL IMAGING, 18(11), 1999.

[20] Hava Lester and Simon R. Arridge. A survey of hierarchical non-linear medical image registration. Pattern Recognition, 32(1):129{149, jan 1999.

[21] Jiayi Ma, Ji Zhao, Yong Ma, and Jinwen Tian. Non-rigid visible and infrared face registration via regularized Gaussian _elds criterion. Pattern Recognition, 48(3):772{784, 2015.

[22] Y. Sun and N. Thakor. Photoplethysmography revisited: from contact to noncontact, from point to imaging. IEEE Transactions on Biomedical Engineering, 63(3):463–477, 2015.

[23] J B Antoine Maintz and Max A Viergever. A survey of medical image registration. Medical Image Analysis, 2(1):1{36, 1998.

[24] David Mattes, David R. Haynor, Hubert Vesselle, Thomas K. Lewellyn, and William Eubank. <title>Nonrigid multimodality image registration</title>. pages 1609{1620, jul 2001.

[25] Nadica Miljkovic, Vladimir Matic, Sabine Van Hu_el, and Mirjana B. Popovic. Independent Component Analysis (ICA) methods for neonatal EEG artifact extraction: Sensitivity to variation of artifact properties. In 10th Symposium on Neural Network Applications in Electrical Engineering, pages 19{21. IEEE, sep 2010.

[26] Jan Modersitzki. Numerical Methods for Image Registration. Oxford University Press, dec 2003.

[27] Yu B Monakhova, S P Mushtakova, S S Kolesnikova, and S A Astakhov. Chemometrics-assisted spectrophotometric method for simultaneous determination of vitamins in complex mixtures.

[28] Ganesh R. Naik. A comparison of ICA algorithms in surface EMG signal processing. International Journal of Biomedical Engineering and Technology, 6(4):363, 2011.

[29] Eddie Y.-K. Ng and Eddie Y.-K. Is thermal scanner losing its bite in mass screening of fever due to SARS? Medical Physics, 32(1):93{97, dec 2004.

[30] Eddie Y.K Ng, G.J.L Kawb, and W.M Chang. Analysis of IR thermal imager for mass blind fever screening. Microvascular Research, 68(2):104{109, 2004.

[31] Jorge. Nocedal and Stephen J. Wright. Numerical optimization. Springer, 2006.

[32] A. K. Noulas and B. J. A. Krose. EM detection of common origin of multimodal cues. In Proceedings of the 8th international conference on Multimodal interfaces - ICMI '06, page 201, New York, New York, USA, 2006. ACM Press.

[33] Nowak, Magdalena Lewandowska, Jacek Rumi_nski, Tomasz Kocejko, and J_edrzej. Measuring pulse rate with a webcam; A non-contact method for evaluating cardiac activity. 2011 Federated Conference on Computer Science andInformation Systems (FedCSIS), (ISBN 978-83-60810-22-4):405{410, 2011.

[34] M Pettersson and A Strandell. [Temperature measurements in health care{a question of quality assurance]. Lakartidningen, 97(37):4050, sep 2000.

[35] Josien P W Pluim, J B Antoine Maintz, and Max A Viergever. Mutual- Information-Based Registration of Medical Images: A Survey. IEEE TRANS-ACTIONS ON MEDICAL IMAGING, 22(8), 2003.

[36] Ming-Zher Poh, Daniel J. McDu_, and Rosalind W. Picard. Non-contact, automated cardiac pulse measurements using video imaging and blind source separation. Optics Express, 18(10):10762, may 2010.

[37] Ming-Zher Poh, Daniel J Mcdu_, and Rosalind W Picard. Advancements in Noncontact, Multiparameter Physiological Measurements Using a Webcam. IEEE TRANSACTIONS ON BIOMEDICAL ENGINEERING, 58(1), 2011.

[38] Ming-Zher Poh, Daniel J McDu_, Rosalind W Picard, S Cook, M Togni, M C Schaub, P Wenaweser, and O M Hess. Non-contact, automated cardiac pulse measurements using video imaging and blind source separation.

[39] Ming-Zher Poh, Nicholas C. Swenson, and Rosalind W. Picard. Motion-tolerant magnetic earring sensor and wireless earpiece for wearable photoplethysmography. IEEE Transactions on Information Technology in Biomedicine, 14(3):786{794, may 2010.

[40] E F J Ring. New standards for fever screening with thermal imaging systems. In Infrared Imaging. IOP Publishing, 2014.

[41] D.N. Rutledge and D. Jouan-Rimbaud Bouveresse. Independent Components Analysis with the JADE algorithm. TrAC Trends in Analytical Chemistry, 50:22{32, 2013.

[42] Christopher G Scully, Jinseok Lee, Joseph Meyer, Alexander M Gorbach, Domhnull Granquist-Fraser, Yitzhak Mendelson, and Ki H Chon. Physiological parameter monitoring from optical recordings with a mobile phone. IEEE transactions on bio-medical engineering, 59(2):303{6, feb 2012.

[43] J.-P. Thirion. Image matching as a di_usion process: an analogy with Maxwell's demons. Medical Image Analysis, 2(3):243{260, sep 1998.

[44] Birgit K. van Staaij, Maroeska M. Rovers, Anne G. Schilder, and Arno W. Hoes. Accuracy and feasibility of daily infrared tympanic membrane temperature measurements in the identi_cation of fever in children. International Journal of Pediatric Otorhinolaryngology, 67(10):1091{1097, oct 2003.

[45] Wim Verkruysse, Lars O Svaasand, and J Stuart Nelson. Remote plethysmographic imaging using ambient light. Optics Express, 16(26):21434, dec 2008.

[46] P. Viola and M. Jones. Rapid object detection using a boosted cascade of simple features. In Proceedings of the 2001 IEEE Computer Society Conference on Computer Vision and Pattern Recognition. CVPR 2001, volume 1, pages I{511{I{518. IEEE Comput. Soc.